

Interstitial trapping and detrapping in electron irradiated dilute copper alloys

To cite this article: F Dworschak *et al* 1975 *J. Phys. F: Met. Phys.* **5** 400

View the [article online](#) for updates and enhancements.

You may also like

- [Optimising Electrochemical Properties of Spinel \$\text{LiMn}_2\text{O}_4\$ Cathode Materials for Lithium Ion Battery Using Microwave Irradiation](#)
Funeka Phumzile Nkosi and Kenneth I. Ozoemena
- [Effect of Gamma Irradiation on DC Performance of Circular-Shaped AlGaIn/GaN High Electron Mobility Transistors](#)
Ya-Hsi Hwang, Yueh-Ling Hsieh, L Lei et al.
- [Radiation-Induced DC Parametric Degradation of Enhancement Mode GaN-\(111\)Silicon High-Electron-Mobility Transistors](#)
Yizhou Lu and Aristos Christou

Interstitial trapping and detrapping in electron irradiated dilute copper alloys

F Dworschak, R Lennartz and H Wollenberger

Van de Graaff-Labor, Aachen der KFA Jülich, Germany and Institut für Allgemeine Metallkunde und Metallphysik der TH Aachen, Germany

Received 5 August 1974, in final form 14 October 1974

Abstract. The interaction of migrating copper interstitials with impurities has been investigated by damage rate measurements in dilute copper alloys with Au, Be, Ge, Ni, Pd, Sb, Zn at irradiation temperatures between 50 and 170 K. By applying the diffusion theory of the three dimensionally migrating interstitial to the data, the resistivity contribution of trapped interstitials and the capture radii of impurities for migrating interstitials has been determined. The above mentioned resistivity contribution was found to be independent of the impurity species and of irradiation temperature. The capture radii of all impurities decrease with increasing irradiation temperature and become zero at about 110 K except that of Be. From the coincidence of this temperature with that of a recovery stage, we conclude this recovery stage to be caused by detrapping of interstitials. The continuous decrease of the capture radii with increasing temperature starting already from 50 K is explained by radiation induced detrapping. The cross section of a trapped interstitial to become detrapped is about 10^6 barn.

1. Introduction

The interaction of radiation induced interstitials with impurities determines the defect retention above the recovery stage I. Interstitials becoming mobile in the temperature range of stage I can be trapped by impurities and hence cannot recombine with vacancies. Defect interactions are also responsible for the stabilization of defects and structure of agglomerates produced by reactor irradiation at high temperatures. Hence, the desired quantitative understanding of a final damage structure requires a quantitative understanding of the defect interactions. The interaction between impurities and migrating interstitials can be determined quantitatively by damage rate measurements as a function of the radiation induced defect concentration. By this method the impurity interstitial interaction in copper has already been studied by Kraut *et al* (1971) for Au, Mn, Ni, and Sb as impurities and at the temperature of 80 K.

In the present paper the study of this interaction is extended to more elements acting as impurities and to different irradiation temperatures. By choosing more impurity elements more information about the origin of the interaction forces was expected to be gained. The investigated temperature range coincides mainly with that of stage II recovery. Stage II recovery has been assigned to impurity effects already by the pioneers in

the radiation damage field (for a review see Corbett 1966). Recovery measurements, however, were not able to give a unique answer to the question of the origin of stage II recovery (Dworschak *et al* 1973). The determination of the impurity interstitial interaction by damage rate measurements within stage II should yield a more detailed knowledge of the processes occurring in the stage II region. Therefore, damage rate measurements have been performed in dilute alloys containing the impurities Au, Be, Ge, Ni, Pd, Sb, Zn at irradiation temperatures between 50 and 170 K. The data are evaluated by using the formalism of the diffusion model for the three dimensionally migrating interstitial (Dworschak *et al* 1968a, 1968b, Kraut *et al* 1971) but considering also higher order effects (Schroeder and Heidrich 1973) which enhance the initial damage rates in dilute alloys above that in the host material. An evaluation according to the off-line crowdion model (Gösele and Frank 1974) leads to the same qualitative but not quantitative results with regard to the interstitial impurity interaction. This off-line crowdion model, however, cannot account for the above mentioned higher order effects.

Fitting our model calculations to the data yields the capture radii of the different impurities for migrating copper interstitials as a function of temperature as well as the resistivity contribution of copper interstitials trapped at the different impurities. The influence of interstitial trapping on the resistivity contribution of interstitials is discussed in detail. The temperature dependence of the capture radii is compared with the recovery behaviour of dilute alloys. This comparison leads to significant conclusions regarding the stability of interstitial impurity complexes against low energy collision events.

2. Experimental

2.1. Samples

The dilute alloys investigated are listed in table 1. All alloys but Cu-Be, Cu-Ge, and Cu-Ni have been supplied[†] in form of 5 mm or 3 mm diameter rods. The Cu-Be alloys were obtained by melting a Cu + 4 weight % Be alloy[‡] packed inside a block of

Table 1. Composition, measured and calculated residual resistivity of the dilute alloys

Alloy	Solute concentration [at ppm]	Residual resistivity	
		Measured [$10^{-9} \Omega\text{cm}$]	Calculated ^a [$10^{-9} \Omega\text{cm}$]
Cu + Au	112	9.7	9.6
+ Be	57	5.2	6.5
+ Be	103	9.0	9.5
+ Be	202	17.0	16.0
+ Ge	200	62.0	70.0
+ Ni	900	103.0	102.0
+ Pd	288	29.5	31.0
+ Sb	255	137.0	138.0
+ Zn	1600	41.5	47.0

^a According to Blatt (1957).

[†] Supplier: Ledgemont Laboratory, Kennecott Copper Corp., Lexington, Mass.

[‡] Supplier: Vakuumschmelze GmbH, Hanau.

99.999% ASARCO copper in an induction furnace under vacuum conditions ($< 1 \times 10^{-4}$ Torr). The Cu-Ni alloy was produced by melting a copper + 1 at % Ni alloy† and 99.999% ASARCO copper in graphite crucibles of high purity under vacuum conditions ($< 5 \times 10^{-5}$ Torr).

All alloys were rolled to foils of 40–70 μm thickness. After every rolling process, the foils were carefully rinsed in benzene, acetone, HNO_3 , HCl and distilled water.

The samples were punched out of these foils, etched in the manner described above and then chemically polished in a mixture of 60% H_3PO_4 , 25% CH_3COOH and 15% HNO_3 . After annealing for 3 h at 700 K under vacuum condition ($< 5 \times 10^{-6}$ Torr) the samples were mounted onto the tail of a continuous flow helium cryostat similar to that one described by Dworschak *et al* (1970).

2.2. Irradiation conditions

The irradiations were performed with 3 MeV electrons. The electron beam density of the Van de Graaff accelerator was homogenized by a magnetic lens system, and by scanning the beam horizontally (999 Hz) and vertically (50 Hz) by sinusoidal magnetic deflection. The beam was then collimated by a set of apertures carefully aligned with the sample area to be irradiated. The electron flux density ($100 \mu\text{A cm}^{-2}$) was homogenous within $\pm 5\%$ across the irradiated area. The absolute uncertainty of the electron dose measurement was about $\pm 5\%$. The maximum temperature difference across each of the

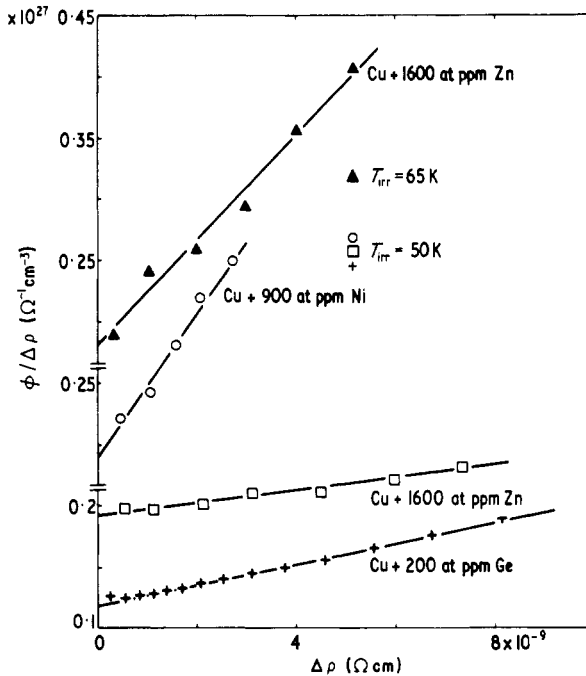


Figure 1. Electron fluence per radiation induced residual resistivity increase as a function of radiation induced residual resistivity increase for various dilute copper alloys and irradiation temperatures. The ordinate origins are shifted by different amounts for the different irradiation temperatures. Within each figure the ordinate scaling is equal for all irradiation temperatures.

† Supplier: Institut für Metallforschung, Technische Universität Berlin.

samples was less than 5 K during irradiation. The samples were irradiated at different temperatures between 50 and 173 K. The electrical resistivity was measured at 4.2 K using standard potentiometric methods. The uncertainty of the resistivity measurements was $\pm 5 \times 10^{-12} \Omega\text{cm}$.

3. Data analysis and results

As has been shown earlier (Dworschak *et al* 1968a, 1968b, Kraut *et al* 1971) the resistivity damage rate in well annealed dilute alloy samples measured under stationary conditions of interstitial diffusion can be written as

$$\frac{d\rho}{d\phi} = f\sigma_d^m \rho_F^i \frac{r_i c_i \rho_F^i}{r_i c_i \rho_F^i + r_v \Delta\rho} \tag{1}$$

where f is the fraction of interstitials escaping correlated recombination, σ_d^m is the displacement cross section of freely migrating interstitials, ρ_F^i is the resistivity increment per unit concentration of Frenkel defects (vacancies and trapped interstitials), r_i and r_v are the capture radii of spherical capture volumes of impurity traps and vacancies, respectively, for migrating interstitials, c_i is the concentration of impurities and $\Delta\rho$ is the radiation induced residual resistivity increase. By assuming only $\Delta\rho$ to depend on ϕ ,

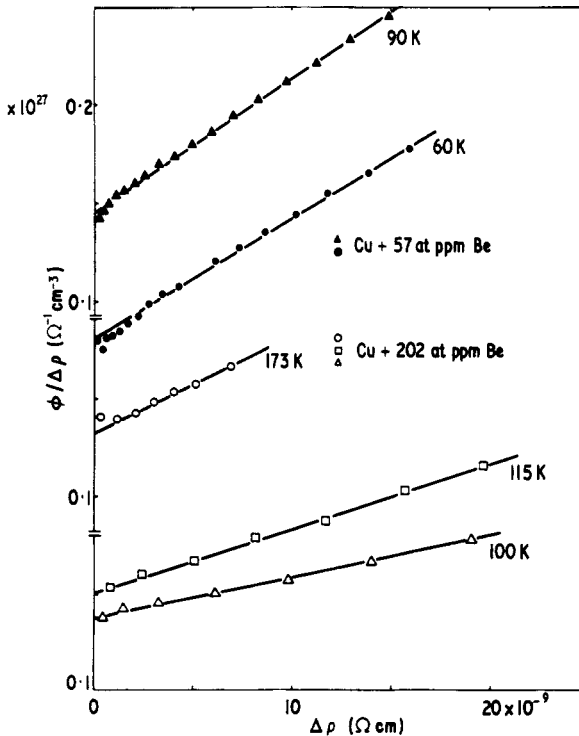


Figure 2. As for figure 1.

integration of equation (1) yields a quadratic relation between ϕ and $\Delta\rho$. It can be written in the form

$$\frac{\phi}{\Delta\rho} = \frac{1}{f\sigma_d^m\rho_F^L} \left(1 + \frac{\Delta\rho}{2c_i\rho_F^L r_i/r_s} \right) \tag{2}$$

which is convenient for a least mean square fit to the damage production data. A least mean square fit of equation (2) to data yields considerably smaller error limits for the wanted parameter r_i/r_s than fitting equation (1) to data. This is due to the much smaller experimental error of the integral quantity $\phi/\Delta\rho$ than the differential one $d\phi/d\rho$. Hence, the data are presented in figures 1-6 in $\phi/\Delta\rho$ against $\Delta\rho$ plots with the irradiation temperature as parameter. In case one of the parameters in equation (1) depends in an unknown manner on ϕ equation (1) cannot be integrated analytically. Therefore, data which do not follow straight lines in $\phi/\Delta\rho$ against $\Delta\rho$ plots are shown in $d\phi/d\rho$ against $\Delta\rho$ plots according to equation (1) in figure 7-9.

The results of fitting equations (1) and (2) to the data are compared with the recovery behaviour of the dilute alloys in §4. The recovery of samples of Cu (99.999% purity,

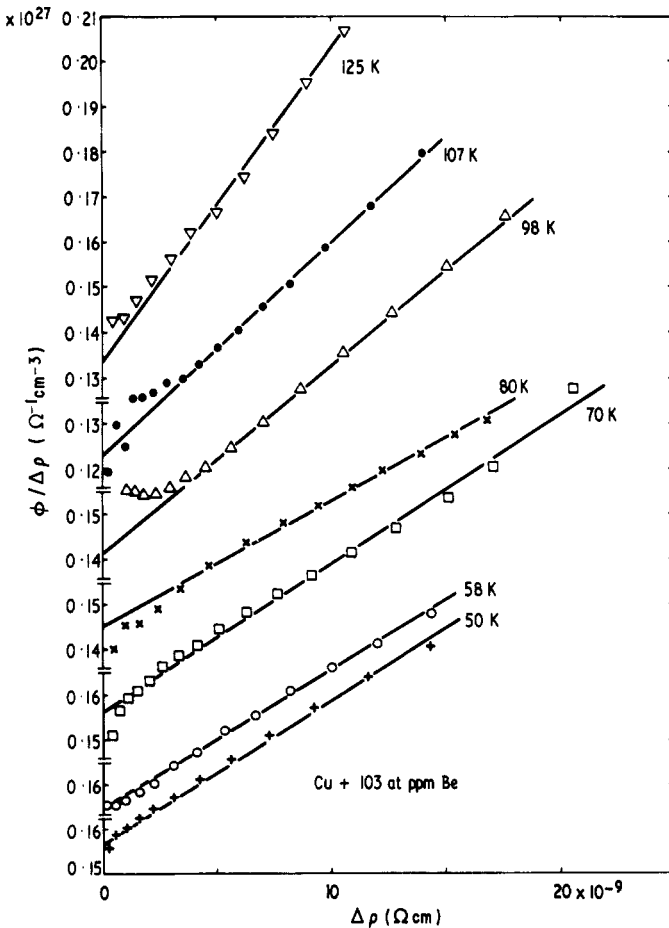


Figure 3. As for figure 1.

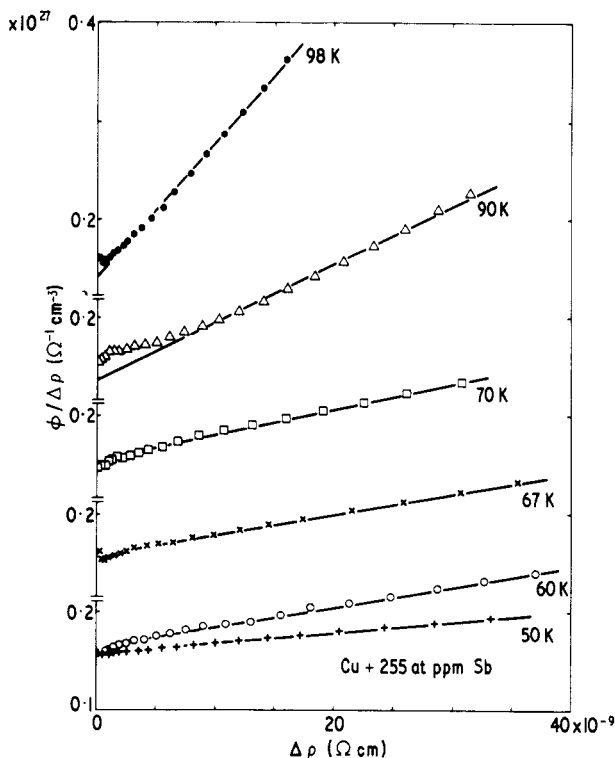


Figure 4. As for figure 1.

ASARCO), Cu + 112 at ppm Au, Cu + 255 at ppm Sb, and Cu + 336 at ppm Ni after irradiation with 3 MeV electrons at 15 K has been investigated in the temperature range 40–110 K by Kraut (1972). The results of the isochronal annealing (periods of ten minutes at each annealing temperature) are shown in figure 10. The residual resistivities ρ_0 and the resistivity increments $\Delta\rho_0$ induced by irradiation with 3 MeV electrons at 15 K are given in table 2.

4. Discussion

4.1. Resistivity contribution of trapped interstitials

Fitting equation (1) or (2) to the data in figures 1–9 yields for each curve $\rho_F^i f \sigma_d^m$ and $\rho_F^i c_i r_i / r_v$ independent of each other. From the curves in figures 7–9 the value of $\rho_F^i c_i r_i / r_v$ is taken for vanishing defect concentration, ie for vanishing $\Delta\rho$.

For a determination of the absolute values of the capture radii it is important to know how ρ_F^i , the resistivity contribution of trapped interstitials and isolated vacancies, is related to the known ρ_F (Ehrhart and Schlagheck 1974) valid for Frenkel defects consisting of isolated vacancies as well as isolated interstitials as they are produced at low temperature (4.2 K) electron irradiation. For pure Cu this relation can be obtained by comparing the fraction of stage I_D annealing to the ratio of damage rates measured below stage I_D and above stage I_E . According to Waite (1957) and Schroeder (1973) the fraction of defects annealing in stage I_D is given by $\langle r_v / r_p \rangle$ (number of defects at the

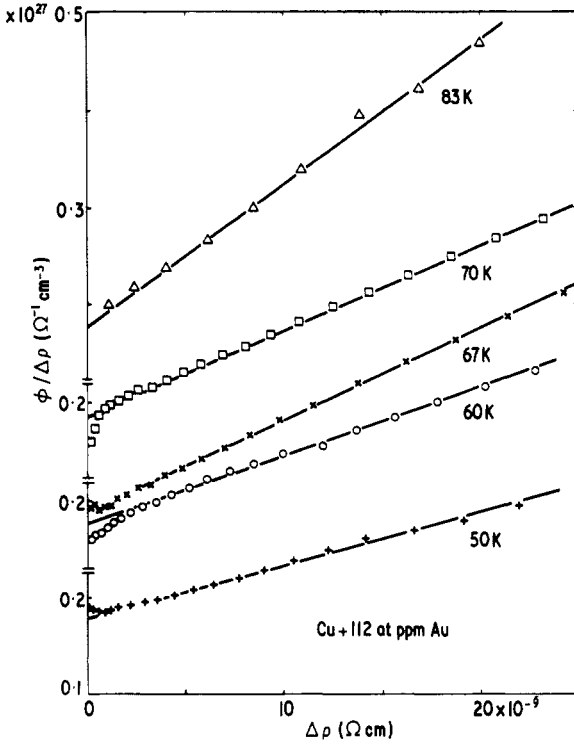


Figure 5. As for figure 1.

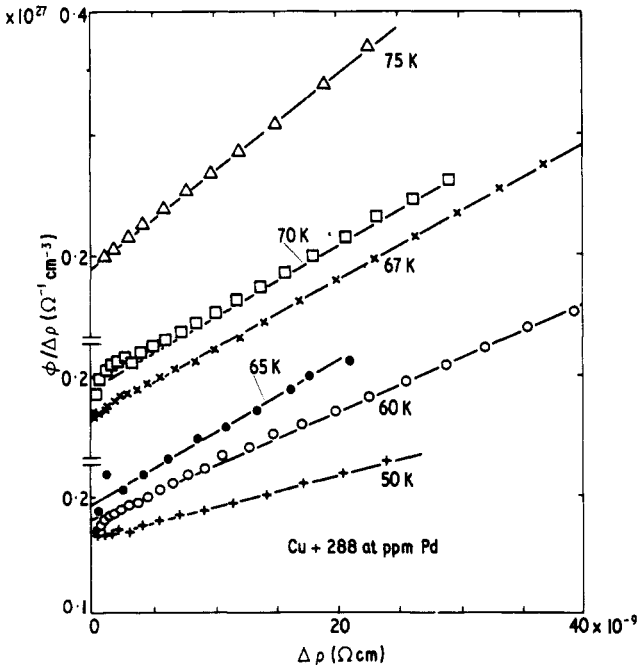


Figure 6. As for figure 1.

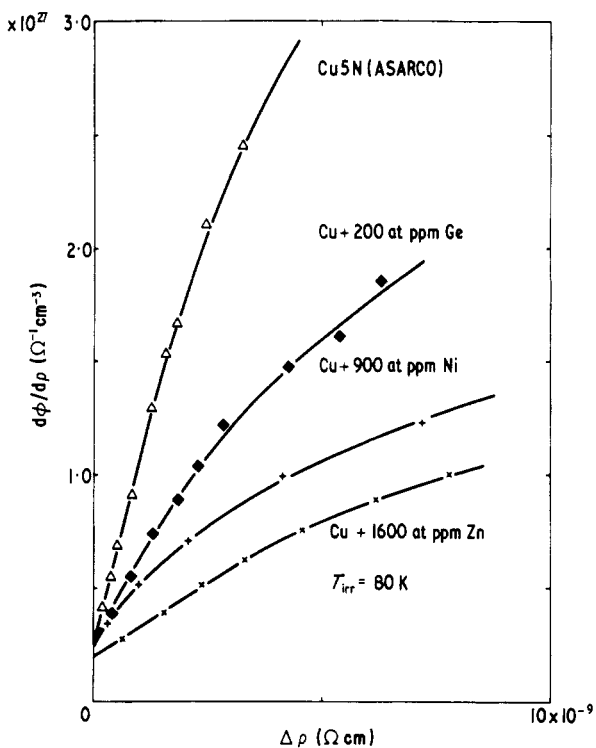


Figure 7. Reciprocal values of damage rates as function of the radiation induced residual resistivity for pure copper and various dilute copper alloys and irradiation temperatures. In figures 8 and 9 the ordinate origins are shifted by different amounts for the different irradiation temperatures and alloys. Within each figure the ordinate scaling is equal for all irradiation temperatures.

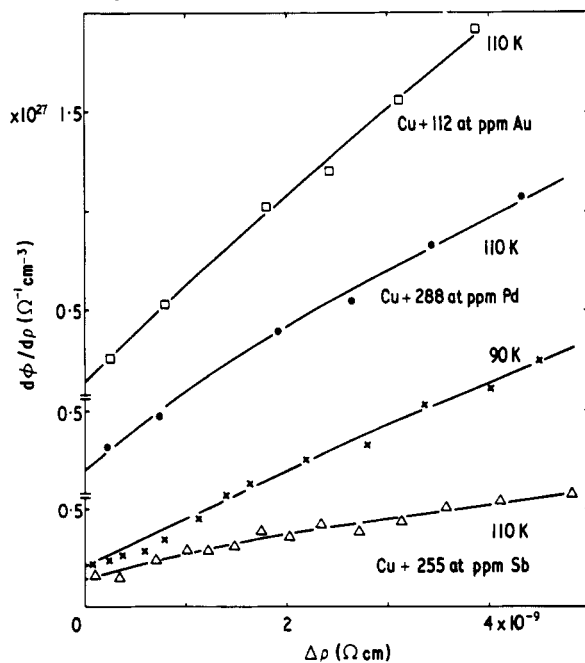


Figure 8. As for figure 7.

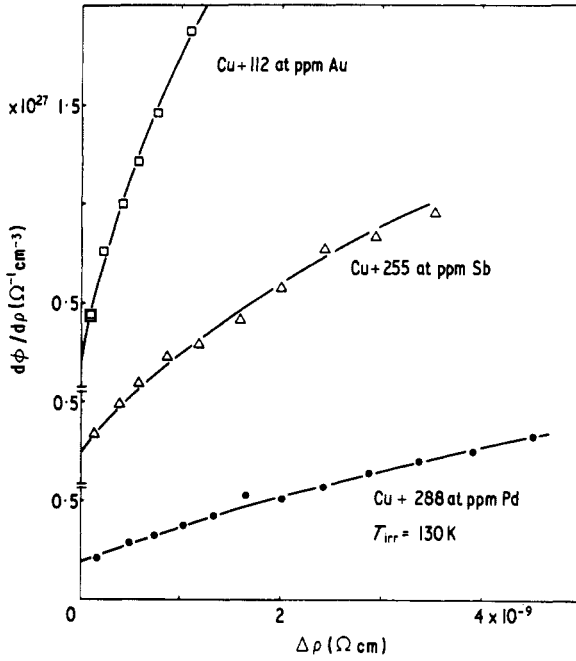


Figure 9. As for figure 7.

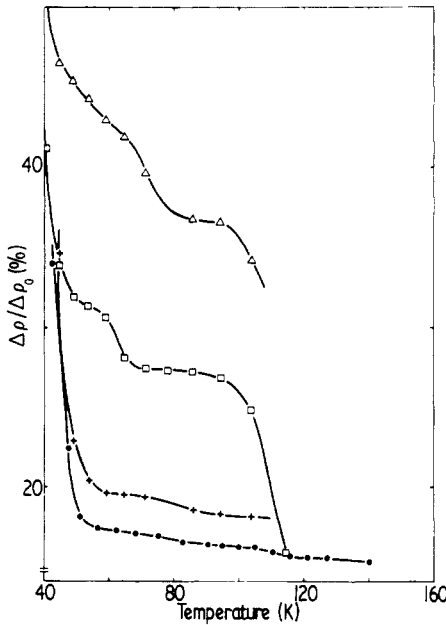


Figure 10. Isochronal recovery of the resistivity of pure copper and dilute copper alloys irradiated at 15 K with 3 MeV electrons. Annealing periods of ten minutes at each temperature. Δ . Cu + 225 at ppm Sb; \square . Cu + 112 at ppm Au; + Cu + 336 at ppm Ni; \bullet . Cu 5N (ASARCO).

Table 2. Composition, residual resistivities and radiation induced resistivities of pure copper and some copper alloys

Alloy	Solute concentration [at -ppm]	Residual resistivity [$10^{-9} \Omega\text{cm}$]	Radiation induced resistivity [$10^{-9} \Omega\text{cm}$]
Cu 5 N(ASARCO)	—	1.8	11.5
Cu + Au	112	12.13 ^a	5.3
+ Ni	336	43.15	18.8
+ Sb	255	157.4 ^a	16.6

^a Samples have been annealed for two h at 700 K in He filled quartz ampullae.

beginning of stage I_D taken to be 100%) with r_v the capture radius of a spherical recombination volume of vacancies for migrating interstitials and r_p the displacement distance. Since Frenkel defects consist of isolated vacancies and isolated interstitials at the beginning as well as at the end of stage I_D , ρ_F does not change during stage I_D annealing. Hence, $\langle r_v/r_p \rangle$ is equal to the fractional resistivity annealing in stage I_D . For sufficiently low defect concentrations stages I_D and I_E are well separated and $\langle r_v/r_p \rangle$ can be determined with good accuracy. From two different experiments the same value $\langle r_v/r_p \rangle = 0.66$ was obtained (Corbett *et al* 1959a, 1959b, Thompson and Sosin 1974). For the ratio of the initial damage rates at 4.2 K and 50 K one obtains

$$\left(\frac{d\rho}{d\phi}\right)_{4.2\text{K}}(0) / \left(\frac{d\rho}{d\phi}\right)_{50\text{K}}(0) = \frac{\sigma_d \rho_F}{f \sigma_d^m \rho_F^l} = \frac{\sigma_d \rho_F}{\sigma_d (1 - f_{\text{ABC}}) (1 - \langle r_v/r_p \rangle) \rho_F^l} \quad (3)$$

with σ_d the displacement cross section at 4.2K and f_{ABC} the fractional annealing in stages I_A - I_C and $f = 1 - \langle r_v/r_p \rangle$. Rewriting equation (3) one obtains

$$\frac{\rho_F^l}{\rho_F} = \frac{1}{(1 - f_{\text{ABC}}) (1 - \langle r_v/r_p \rangle)} \frac{(d\rho/d\phi)_{50\text{K}}(0)}{(d\rho/d\phi)_{4.2\text{K}}(0)}$$

The ratio $\langle r_v/r_p \rangle$ was found by Becker *et al* (1972) to have a $T^{-1.3}$ dependence. The $\langle r_v/r_p \rangle$ value from annealing experiments corresponds to 45 K (end of stage I_D) (Corbett *et al* 1959a, 1959b). From $\langle r_v/r_p \rangle = 0.66$ at 45 K one obtains 0.64 for 50 K. Using $f_{\text{ABC}} = 0.23$ (Schilling *et al* 1970) and the initial damage rates reported by Becker *et al* (1972) one obtains

$$\rho_F^l / \rho_F = 1.05 \pm 0.16.$$

This value agrees within the experimental errors with 0.8 ± 0.1 as derived by Thompson *et al* (1973). The resistivity contribution ρ_F^l consists of that of the trapped interstitials and of the isolated vacancies. The contribution of the isolated vacancy is expected to be independent of the impurity species whereas that of the trapped interstitials could be influenced. A dependence of ρ_F^l upon the different impurity species can be found by comparing the quantity $\rho_F^l f \sigma_d^m$ measured in a dilute alloy at a certain temperature with that measured by Becker *et al* (1972) in pure Cu at the same temperature. Before doing this, we have to ensure whether the impurities can influence the values of σ_d^m and f , respectively.

The cross section σ_d^m should be the same as in pure Cu since it describes the interaction of the irradiating particle with lattice atoms. The fraction of about 100 ppm impurities among the lattice atoms can have only a negligible influence on the cross section. The fraction f , however, is different for pure Cu and the dilute alloys since $f = 1 - \langle r_v/r_p \rangle$ is a good approximation only as long as $\frac{4}{3}\pi r_1^3 c_1 \ll 1$ holds. The exact solution has been given by Schroeder and Heidrich (1973) to be

$$f = 1 - \frac{r_v}{r_p} 2 \left(\frac{A}{\pi} \right)^{1/2} \sum_{m \geq 0} \frac{(-2B\sqrt{A})^m}{m!} K_{(m-1)/2}(2A) \quad (4)$$

with

$$A = (\pi \bar{R} \bar{C})^{1/2} (r_p - r_v) \quad B = (4\bar{R}^3 \bar{C})^{1/2}$$

$$\bar{R} = \frac{r_1^2 c_1 + r_v^2 c_v}{r_1 c_1 + r_v c_v} \quad \bar{C} = \frac{(r_1 c_1 + r_v c_v)^2}{r_1^2 c_1 + r_v^2 c_v}$$

$K_\nu(x)$ are modified Bessel functions of the 3rd kind.

In deriving equation (4) a δ distribution of displacement distances r_p was assumed whereas at least two different values of r_p were needed to sufficiently explain the observed energy dependence (Becker *et al* 1973). A Gaussian initial distribution has been found to provide an adequate fit to stages I_D - I_E recovery data by Corbett *et al* (1959b) and by Thompson and Sosin (1974). All these different distributions produce virtually the same final recovery values. Equation (4) yields about the same result for f when it is calculated as a weighted average of two f 's valid for two different r_p 's or when it is calculated for the averaged r_p .

In equation (4) the radii r_v and r_p must be the same in the dilute alloys as in pure Cu for the same reasons given for the equality of σ_d^m . The absolute value of r_v was derived from annealing experiments by Thompson and Sosin (1974) to be 3.2 ± 0.3 lattice distances at 50 K. The trapping radius r_1 can be derived from the term $\rho_F r_1 c_1 / r_v$ resulting from the fitting procedure by assuming ρ_F to be independent on temperature and equal to $2.5 \times 10^{-4} \Omega\text{cm}$. The trapping concentration c_1 equals the impurity content as obtained from chemical analysis. Now by using equation (4) f^{alloy} can be calculated. For the numerical evaluation of the dependence of the initial damage rate on $r_1 c_1$ the graphic representation given in figure 14 of the paper by Heidrich (1973) has been used with

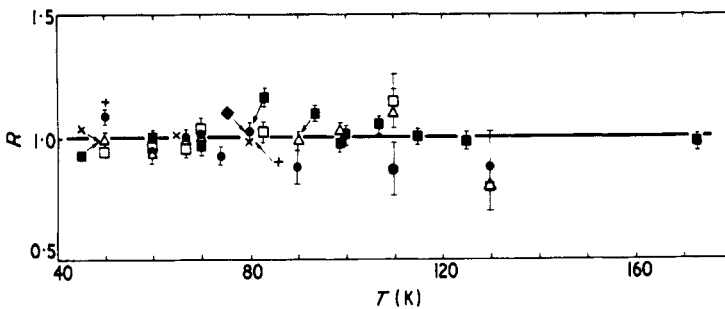


Figure 11. The ratio of resistivity contribution per unit concentration of Frenkel defects in dilute copper alloys to that in pure copper as a function of irradiation temperature (◆, Ge; ■, Be; ●, Pd; △, Sb; □, Au; +, Ni; ×, Zn).

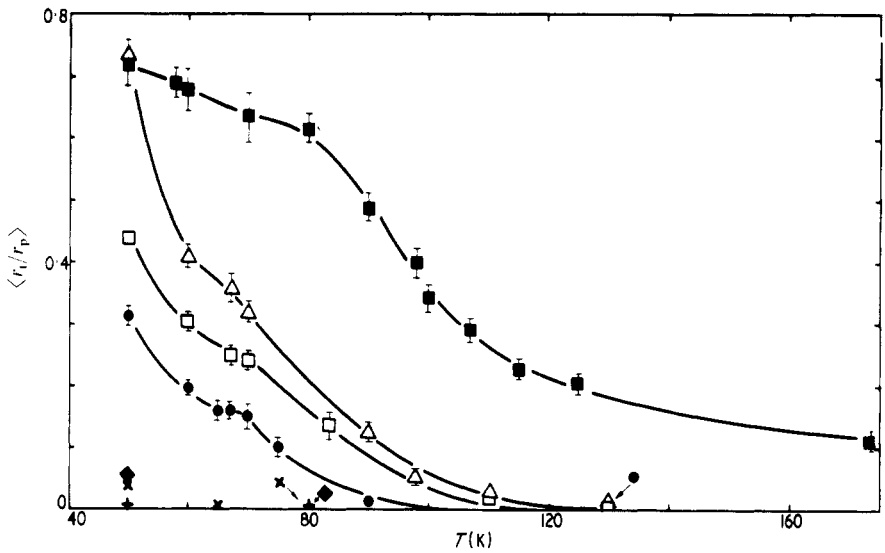


Figure 12. Temperature dependence of the capture radius of different impurities for migrating copper interstitials. \blacklozenge , Ge; \blacksquare , Be; \bullet , Pd; \triangle , Sb; \square , Au; $+$, Ni; \times , Zn.

the parameter $r_p = 2.0 r_i$. Dividing the initial damage rate measured in a dilute alloy at a certain temperature by that measured in pure Cu at the same temperature and multiplying by f^{Cu}/f^{alloy} yields

$$R = \frac{(d\rho/d\phi)^{alloy}(0)}{(d\rho/d\phi)^{Cu}(0)} \frac{f^{Cu}}{f^{alloy}} = \frac{\rho_F^{alloy} f^{alloy} \sigma_d^m f^{Cu}}{\rho_F^{Cu} f^{Cu} \sigma_d^m f^{alloy}} = \frac{\rho_F^{alloy}}{\rho_F^{Cu}}$$

the ratio of resistivity contribution per unit concentration of Frenkel defects in an alloy to that in pure Cu. From the initial damage rates for pure Cu (Becker *et al* 1972) and those obtained by fitting equation (2) to the data in figures 1–6 and by fitting equation (1) to the data in figures 7–9, we obtain R as function of irradiation temperature as shown in figure 11. The error bars give the standard deviations obtained from the least mean square fits of equation (2) to the data in figures 1–6. It should be mentioned that two or three irradiation runs have been performed for many irradiation temperatures and most of the alloys. The scattering of the fitting results for one and the same irradiation temperature and alloy lies within the error bars shown in figures 11 and 12. For the data in figures 7–9 the ordinate intercepts have been obtained by graphic extrapolation. Here the error bars indicate the estimated uncertainty of the graphic extrapolation. According to the results in figure 11 the resistivity contribution of interstitials trapped at Au, Be, Ge, Ni, Pd, Sb and Zn is equal within the experimental error to that of interstitials trapped by the residual impurities of pure Cu containing the ‘natural’ residual impurities (Le Hérycy 1966). This result indicates that the residual impurities behave as the impurities investigated in the present alloys.

Within the frame of the off-line crowdion model treated by Gösele and Frank (1974) the enhancement of the initial damage rates observed here must be ascribed to an enhancement of the ρ_F^i or ρ_F^{alloy} , respectively, alone, since the model does not account for an influence of impurity traps on the correlated recovery. Quantitatively the ratio $\rho_F^{alloy}/\rho_F^{Cu}$ turns out to be 1.4 for most of the impurities. Then the resistivity contribution of

the trapped interstitial must be about twice that of an interstitial trapped at a residual natural resistivity which can hardly be understood. Of course, the crowdion model can be satisfactorily adjusted to the experimental data by adding an appropriate fraction of on-line crowdions to the off-lines.

4.2. Temperature dependence of the capture radii

As described in § 4.1 fitting of equation (1) or (2) to the data in figures 1–9 yields $\rho_F^{\dagger} c_i r_i / r_v$. With $\rho_F^{\dagger} = 2.5 \times 10^{-4} \Omega\text{cm}$ and the c_i values obtained from chemical analysis one gets r_i / r_v as a function of temperature. The temperature dependence of $\langle r_i / r_p \rangle$ was found by Becker *et al* (1972) to be proportional to $T^{-1.3}$. The displacement distance r_p of about 5 lattice distances at 3 MeV electron energy (55 eV average recoil energy) should not depend on temperature within the temperature range investigated here, since the average recoil energy is large compared with the thermal energy. Focusing effects which might be temperature dependent should not play any important role because of the relatively large specific energy loss of 55 eV per 5 lattice distances. Hence, the temperature dependence found for $\langle r_i / r_p \rangle$ must be caused by that of r_v and we can eliminate this temperature dependence in r_i / r_v by multiplying this ratio with $\langle r_i / r_p \rangle$ yielding $\langle r_i / r_p \rangle$. The result is shown in figure 12.

For all investigated impurities the ratio r_i decreases with increasing temperature already from the lowest temperature investigated. At lower temperatures than 50 K our method unfortunately cannot be applied. In this temperature range the jump frequency of the interstitials is too small so that the stationary diffusion conditions presumed in deriving equation (1) are not attained within experimental times.

For all impurities investigated except Be r_i becomes negligibly small at temperatures between 100 and 130 K. In this temperature range the product $r_i c_i$ approximates the values observed in pure copper (99.999% ASARCO, residual resistivity $\rho_0 = 2 \times 10^{-9} \Omega\text{cm}$) at 130 K (Becker 1972). The impurities Ge, Ni and Zn lose their trapping ability already at about 60 K. Be obviously preserves its trapping property up to 170 K, the highest temperature investigated.

The temperature range of 100 to 130 K coincides with the recovery stage near 110 K observed by Dworschak *et al* (1973) during isochronal annealing of samples (sample material being the same as in the present work) irradiated at 60 K. It seems quite reasonable to conclude from this coincidence that this recovery stage originates from detrapping of interstitials which subsequently migrate and recombine with vacancies. From the fact that only about 30% recovery occurs at 110 K, we conclude that substantial interstitial clustering takes place during migration of the detrapped interstitials, in agreement with the conclusion of diffuse x ray scattering results (Ehrhart and Schlagheck 1974). The alloy with Be shows negligible recovery at 110 K in accordance with the nonvanishing r_i in figure 12.

The annealing stage around 65 K (figure 10) seems also to be accompanied by a strong decrease of r_i / r_p since a clear two step decrease can be seen in the curves in figure 12. Hence, we assign the recovery stage at 60 K also to a detrapping process. The comparably small recovery of only a few per cent indicates either that this type of trap contributes only to a small fraction of the total trap concentration or that most of the detrapped interstitials are again captured by the deeper trap.

There is an important difference between the recovery behaviour and the temperature dependence of r_i . Almost no recovery was observed between 70 and about 100 K (Dworschak *et al* 1973) whereas r_i decreases drastically in this temperature

range. Obviously, interstitials trapped at 70 K do not escape the trap during isochronal annealing until temperatures of about 110 K are reached. Contrary to this, the probability of interstitials becoming trapped decreases continuously with increasing irradiation temperature between 50 and 130 K. Since the simplest explanation of the continuous decrease of the trapping probability would be a partial thermal activated detrapping during irradiation, we checked the recovery behaviour when the samples are annealed at the irradiation temperature subsequent to a damage rate measurement. At 80 K, for example, the total annihilation amounted to less than 7% (maximum value observed for Cu + Pd) of the last irradiation induced damage increment $\rho_n - \rho_{n-1}$ and less than 1% of the total damage. It should be mentioned that another result could have hardly been understood in view of the isochronal recovery result. Quantitative deviations in isochronal and isothermal annealing experiments would have led to the conclusion that a less stable defect structure is produced during an irradiation at, say, 80 K than by an irradiation at 70 K with subsequent isochronal annealing to 80 K. The main difference between both types of experiments in our case, however, is the electron irradiation acting during the isothermal treatment.

As is well known, defects are not only produced but can also be annihilated by electron irradiation (subthreshold events). Subthreshold collisions were found to induce annihilation of defects which otherwise anneal thermally activated at a temperature somewhat above the irradiation temperature (Wollenberger 1970). If trapped interstitials were detrapped by subthreshold collisions at temperatures below 110 K, at which temperature the thermally activated detrapping occurs, an apparent decrease of the capture radius would be observed. If, furthermore, the amount of subthreshold energy transfer required for detrapping decreases with decreasing distance from the thermal recovery temperature, the cross section (Coulomb scattering) for such events, and hence the apparent reduction of the trapping radius, must increase. Thus, the effective trapping radius decreases with increasing irradiation temperature until it vanishes at the thermal recovery temperature. Obviously, the discrepancy between the temperature dependence of r_t and the isochronal recovery can be explained by an irradiation induced detrapping. On the other hand, it is not obvious why linear $\phi/\Delta\rho$ against $\Delta\rho$ plots are observed although part of the trapped interstitials become mobile again during the irradiation experiment. If all trapped interstitials were equally sensitive to subthreshold collisions the annihilation rate could be proportional to the total defect concentration. This would lead to a nonlinear relation between $\phi/\Delta\rho$ and $\Delta\rho$. Linear relations are to be expected, however, when only a certain fraction of interstitials is trapped in positions being sensitive to radiation induced detrapping and when the cross section for detrapping reaches a certain order of magnitude which is discussed below. To discuss the model in a little more detail, we make the following assumptions. The trapped interstitials being sensitive to athermal (radiation induced) detrapping are produced according to the cross section σ_{ds} and are detrapped according to the cross section σ_a . Then we get the damage rate

$$\frac{d\rho_s}{d\phi} = \rho_F \frac{dc_s}{d\phi} = \rho_F(\sigma_{ds} - \sigma_a c_s) \tag{5}$$

where c_s is the concentration of the sensitive trapped interstitials. The cross section σ_{ds} can be written as

$$\sigma_{ds} = \sigma_d^m f \frac{(r_t c_t)_s}{r_t c_t + r_s c} \tag{6}$$

where $(r_i c_i)_s$ designates those traps in which the interstitials are sensitive to athermal detrapping. According to equation (6) σ_{ds} depends on the total defect concentration c . For small changes of c , however, we can take it constant. With a constant σ_{ds} equation (5) can be integrated and yields

$$\Delta\rho_s = \rho_F c_s = \rho_F \frac{\sigma_{ds}}{\sigma_a} [1 - \exp(-\sigma_a \phi)]. \quad (7)$$

The effect of a mechanism described by equation (5) is illustrated in figure 13. For $\Delta\rho \rightarrow 0$ we have $c_s \rightarrow 0$ and hence, the $\phi/\Delta\rho$ against $\Delta\rho$ curves start with a slope corresponding to the product $r_i c_i$ (c_i is the total effective trap concentration). During a transition period given by the decrease of $\exp(-\sigma_a \phi)$ in equation (7) with increasing ϕ the damage rate $d\rho_s/d\phi$ in equation (5) vanishes. Hence, the $\phi/\Delta\rho$ against $\Delta\rho$ curve in this period approximates a straight line having a slope corresponding to $r_i c_i - (r_i c_i)_s$. The extrapolated ordinate intersect of this straight line coincides with that valid for $\phi = 0$ as a detailed consideration of the rate equations describing the present model shows.

The experimental data in figures 1-7 do generally not show a behaviour as given in figure 13. Sometimes deviations from linearity can be seen for $\Delta\rho$ values smaller than about $2 \times 10^{-9} \Omega\text{cm}$. Sometimes an exact linear behaviour is observed already from the first data point. The reasons for the deviations are not quite clear. During the experimental work no particular importance was attached to the measurement uncertainty at small values of $\Delta\rho$ since the most exact information comes from the data points at large values of $\Delta\rho$. Taking the data as they are, we cannot decide whether effects according to figure 13 do occur or not for $\Delta\rho$ values smaller than $2 \times 10^{-9} \Omega\text{cm}$. Assuming $d\rho_s/d\phi$ (equation (5)) to have become negligibly small at this value of $\Delta\rho$ one can easily estimate the required order of magnitude of σ_a according to equation (7) and to the data points. As a result one obtains $\sigma_a \approx 10^6$ barn.

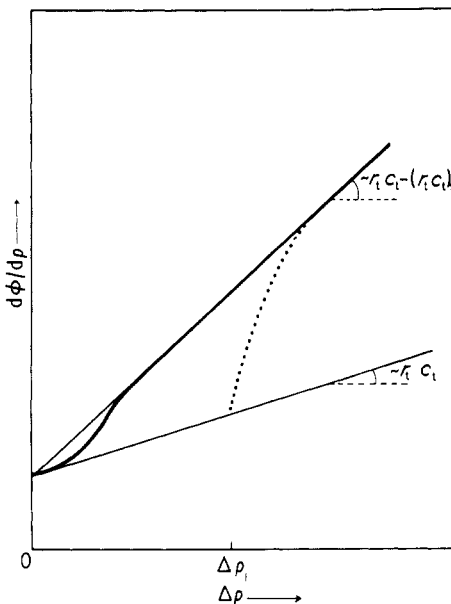


Figure 13. Schematic drawing showing the influence of radiation induced detrapping on the reciprocal damage rate (see text).

How can the existence of such an athermal detrapping be proved? From figure 13 one concludes that a more distinct effect would be expected when it were possible to attain $c_s = 0$ (equation (5)) at a value $\Delta\rho_1$ at which the difference between the two straight lines is well beyond the experimental error. Then the first data point must again lie close to the straight line corresponding to r_1c_1 and the transition period is described by the dotted curve in figure 13. In order to attain $c_s \approx 0$ at $\Delta\rho_1$ one should irradiate at a higher temperature than the one of interest until the wanted $\Delta\rho$ value is reached. Then the irradiation temperature should be lowered to the interesting one and there the inverse damage rate should be measured as function of $\Delta\rho$. According to our initial assumptions σ_a valid for a certain trap position should increase with increasing temperature and hence, $c_s(\phi \rightarrow \infty)$ should decrease. Consequently, after lowering the irradiation temperature c_s will be smaller than its saturation value at this temperature. Whether it is practically zero or not depends on the amount of the temperature dependence of σ_a which is not yet known. To check this model, we have irradiated dilute alloys at 90 K up to $\Delta\rho$ values of about $20 \times 10^{-9} \Omega\text{cm}$ and then have changed the irradiation temperature to 70 K. At this temperature the data points shown in figure 14 were obtained. The straight lines are those obtained from figures 4, 5 and 6 for 70 K irradiation temperature. The data points are obviously in qualitative agreement with our model. The data points deviate from the straight lines by more than the experimental uncertainty only within ranges of about $2 \times 10^{-9} \Omega\text{cm}$ for the alloys with Au and Pd and of about $6 \times 10^{-9} \Omega\text{cm}$ for the alloy with Sb. The difference of the damage rates given by a data point and by the corresponding straight line taken at the same value of $\Delta\rho$ equals $d\rho_s/d\phi$ as given by equation (6). This quantity is plotted logarithmically against ϕ in figure 15. Again the experimental results are in rough agreement with

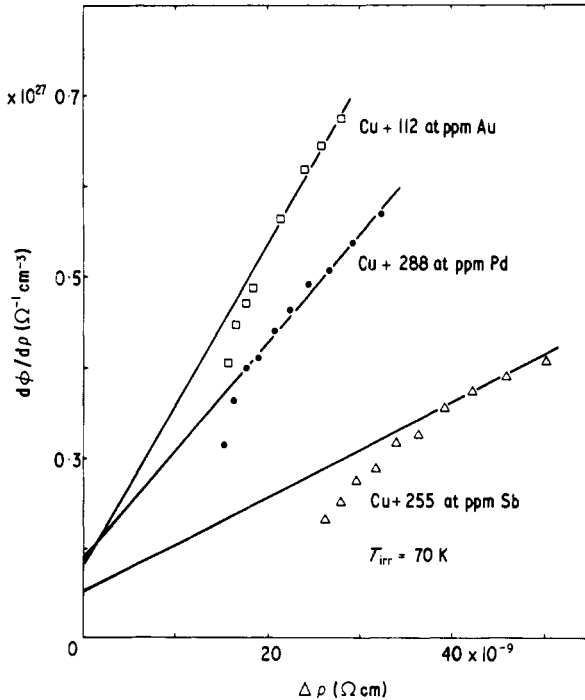


Figure 14. Reciprocal damage rates after pre-irradiation at 90 K for different dilute copper alloys. Straight lines are those obtained from figures 4, 5 and 6.

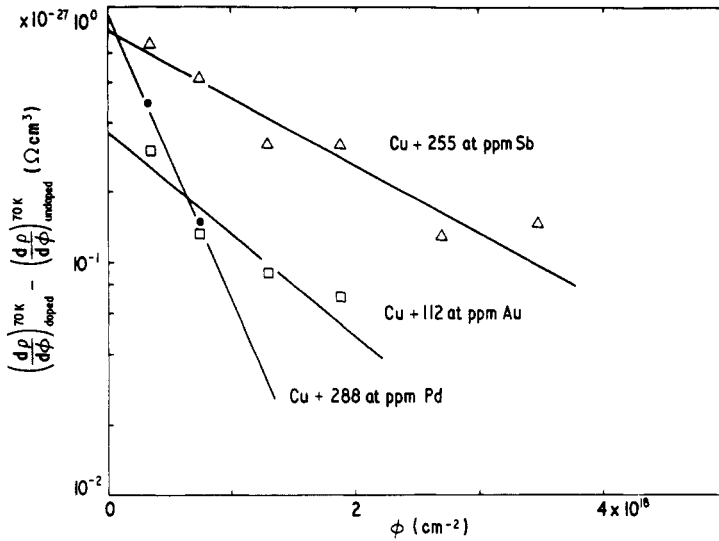


Figure 15. Difference of damage rates of high temperature pre-irradiated (doped) and undoped samples taken at the same value of $\Delta\rho$ as a function of fluence.

equation (6). From the straight lines in figure 15 we obtain for σ_a values of 0.6×10^6 barn, 1×10^6 barn, and 27×10^6 barn for the alloys with Sb, Au, and Pd, respectively.

For radiation induced close pair recombination in Al, Cu and Pt, cross sections in the order of magnitude of 10^4 barn have been found earlier (Wollenberger 1970). They could be explained quantitatively by assuming that a knock on of one of the next neighbouring atoms of a close pair induces recombination when the recoil energy is in the order of magnitude of the thermal activation energy for recombination. Cross sections for defect annihilation in the order of 10^6 barn have been measured recently in Au. It seems quite reasonable to explain these data also by radiation induced detrapping of gold interstitials (Dworschak *et al* 1974). The mechanism of the athermal detrapping, however, is not yet understood. In order to get a total cross section of 10^6 barn by Mott scattering (Mott 1929, 1932) a minimum recoil energy of the interstitial of less than 10^{-3} eV is required. But this energy is below the thermal energy, i.e. such detrapping processes should be thermally activated. To avoid this inconsistency one is forced to conclude that detrapping is already induced when any one of about 100 neighbouring atoms of the interstitial impurity complex receives a recoil energy in the order of magnitude of 0.1 eV. How can such a high sensitivity of an interstitial complex against subthreshold energy transfer come about?

It is true that the resonance mode of the dumb-bell interstitial detected by computer experiments (Dederichs *et al* 1973) leads to small activation energies for migration steps. A quantitative treatment leads nearly to a suitable understanding of the activation energy for interstitial migration of 0.1 eV which is, however, large compared with the small threshold energy required for a quantitative explanation of the athermal detrapping. Since those giant cross sections are always observed when trapped interstitials are involved it seems that they are specific for interstitial impurity complexes. High voltage electron microscopic observations seem to indicate that vacancy migration can also be induced by subthreshold collisions with a very high cross section (Urban 1974).

From the straight lines in figure 15 one obtains $d\rho_s/d\phi$ for $\phi = 0$ to be in the order of magnitude of $10^{-27} \Omega\text{cm}^3$. It is, however, not certain whether the ordinate intercepts in figure 15 are equal to $\rho_F\sigma_{a_s}$ in equation (6) since it is questionable whether the 90 K pre-irradiation really caused c_s to be zero at the beginning of the 70 K irradiation. Probably this is not the case, and therefore $\rho_F\sigma_{a_s}$ will be larger than the ordinate intercepts in figure 15. A detailed investigation of the temperature dependence of σ_a and related questions is under progress.

A quantitative comparison of the experimental values of r_i with results of drift diffusion calculation which consider the elastic interaction between migrating interstitials and impurity (Kraut *et al* 1971) must be postponed until the temperature dependent part of $r_i c_i$ has been determined.

5. Conclusions

Evaluation of the present damage rate data and the annealing data in the literature by means of the diffusion model for the three dimensionally migrating interstitial yields the following results:

- (i) The resistivity contribution of an interstitial trapped at Au, Be, Ge, Ni, Pd, Sb or Zn impurities is, within the experimental uncertainty of about 20%, equal to that of interstitials trapped at the natural residual impurities.
- (ii) The resistivity contribution of an interstitial trapped at the natural residual impurities is, within the experimental uncertainty of 30%, equal to that of an isolated interstitial.
- (iii) The capture radii of all impurities for migrating interstitials decrease with increasing irradiation temperature and become zero at about 110 K except that of Be (figure 12).
- (iv) The result given in (iii) indicates that the annealing stage observed around 110 K is due to thermally activated detrapping.
- (v) Interstitials are detrapped by electron atom collisions with a cross section of about 10^6 barn at an irradiation temperature of 70 K.
- (vi) The temperature dependence of the capture radii is concluded to be caused by a temperature dependence of the cross section given in (v).

Acknowledgments

The authors kindly thank Mr N E Hamilton of Kennecott Copper Corp. and Professor Dr H Wever of Institut für Matallforschung der TU Berlin for supplying them with the alloy material. They wish to thank Dr K Schroeder for many helpful discussions. Many thanks are due to Professor Dr K Lücke for his permanent support and to the staff of the Van de Graaff Laboratory for the valuable assistance during the experiments.

References

- Becker D E 1972 *Berichte der Kernforschungsanlage Jülich-Jül-857*
 Becker D E, Dworschak F and Wollenberger H 1972 *Phys. Stat. Solidi* (b) **54** 455
 — 1973 *Radiation Effects* **17** 25

- Blatt F J *Solid State Physics* vol 4 ed F Seitz and D Turnbull (New York: Academic Press) pp 199–396
- Corbett J W 1966 *Solid State Physics Supplement* vol 7 ed F Seitz and D Turnbull (New York: Academic Press) pp 1–410
- Corbett J W, Smith R B and Walker R M 1959a *Phys. Rev.* **114** 1452 1959b *Phys. Rev.* **114** 1460
- Dworschak F, Holfelder G and Wollenberger H 1974 *Verhandl. DPG (VI)* **9** 767
- Dworschak F, Kraut A, Sonnenberg K and Wollenberger H 1973 *Radiation Effects* **19** 119
- Dworschak F, Neuhäuser J, Schuster H, Wollenberger H and Wurm J 1970 *Rev. Sci. Instrum.* **41** 64
- Dworschak F, Schuster H, Wollenberger H and Wurm J 1968a *Phys. Stat. Solidi* **29** 75
- 1968b *Phys. Stat. Solidi* **29** 81
- Ehrhart P and Schlagheck U 1974 *J. Phys. F: Metal Phys.* **10** 1575–98
- Gösele V and Frank W 1974 *Phys. Stat. Solidi (b)* **61** 163
- Heidrich W 1973 *Berichte der Kernforschungsanlage Jülich–Jül–1006–FF*
- Kraut A 1972 *Berichte der Kernforschungsanlage Jülich–Jül–896–FF*
- Kraut A, Dworschak F and Wollenberger H 1971 *Phys. Stat. Solidi (b)* **44** 805
- Le Héricy J 1966 *Ann. Chim.* **1** 129
- Mott N F 1929 *Proc. R. Soc. A* **124** 426
- 1932 *Proc. R. Soc. A* **135** 429
- Schilling W, Burger G, Isebeck and Wenzl H 1970 *Vacancies and Interstitials in Metals* (Amsterdam: North Holland) pp 255–361
- Schroeder K 1973 *Radiation Effects* **17** 103
- Schroeder K and Heidrich W 1973 *Phys. Lett.* **34A** 315
- Thompson L and Sosin A 1974 to be published
- Thompson L, Youngblood G and Sosin A 1973 *Radiation Effects* **20** 111
- Urban K 1974 *High Voltage Electron Microscopy* (London, New York: Academic Press) p 356
- Waite T R 1957 *Phys. Rev.* **107** 463
- Wollenberger H 1970 *Vacancies and Interstitials in Metals* (Amsterdam: North Holland) pp 215–50